

PACS numbers: 62.20.Qp, 62.23.Pq, 81.05.Mh, 81.05.Ni, 81.20.Ev, 81.40.Ef, 81.40.Lm

## **Influence of Thermal Deformation Treatment Conditions on the Structure and Mechanical Properties of the Fe–Ti–C System**

A. V. Minitzkiy<sup>\*,\*\*</sup>, Ye. S. Shaposhnikova<sup>\*</sup>, Ie. G. Byba<sup>\*,\*\*</sup>,  
N. V. Minitzka<sup>\*,\*\*\*\*</sup>, O. V. Kozlenko<sup>\*</sup>, V. L. Syrovatka<sup>\*\*\*</sup>, D. S. Leonov<sup>\*\*\*\*</sup>,  
and M. Yu. Barabash<sup>\*,\*\*,\*\*\*\*,\*\*\*\*\*</sup>

<sup>\*</sup>*National Technical University of Ukraine  
'Igor Sikorsky Kyiv Polytechnic Institute',  
37 Beresteiskyi Ave.,  
UA-03056 Kyiv, Ukraine*

<sup>\*\*</sup>*Institute for Applied Control Systems, N.A.S. of Ukraine,  
42 Academician Hlushkov Ave.,  
UA-03187 Kyiv, Ukraine*

<sup>\*\*\*</sup>*I. M. Frantsevych Institute for Problems in Materials Science, N.A.S. of Ukraine,  
3 Omeljan Pritsak Str.,  
UA-03142 Kyiv, Ukraine*

<sup>\*\*\*\*</sup>*Technical Centre, N.A.S. of Ukraine,  
13 Pokrovs'ka Str.,  
UA-04070 Kyiv, Ukraine*

<sup>\*\*\*\*\*</sup>*Gas Institute of N.A.S. of Ukraine,  
39, Degtyarivska Str.,  
UA-03113 Kyiv, Ukraine*

The effect of thermal-deformation treatment on the structure and physical and mechanical properties of the Fe–Ti–C metal–ceramic composite material, which is synthesized *in situ* from a Fe–86.0%, Ti–10.0%, and graph-

---

Corresponding author: Anatolii Viacheslavovych Minitzkiy  
E-mail: [aminitsky@gmail.com](mailto:aminitsky@gmail.com)

Citation: A. V. Minitzkiy, Ye. S. Shaposhnikova, Ie. G. Byba, N. V. Minitzka, O. V. Kozlenko, V. L. Syrovatka, D. S. Leonov, and M. Yu. Barabash, Influence of Thermal Deformation Treatment Conditions on the Structure and Mechanical Properties of the Fe–Ti–C System, *Metallofiz. Noveishie Tekhnol.*, **48**, No. 2: 141–151 (2026). DOI: [10.15407/mfint.48.02.0141](https://doi.org/10.15407/mfint.48.02.0141)

© Publisher PH 'Akademperiodyka' of the NAS of Ukraine, 2026. This is an open access article under the CC BY-ND license (<https://creativecommons.org/licenses/by-nd/4.0>)

ite—4.0% powder mixture, is studied. Titanium carbide (TiC) is a reinforcing phase, as it has high hardness (30 GPa), high melting point ( $\cong 3100^\circ\text{C}$ ), and low contact angle with iron ( $\cong 20^\circ$ ) that promotes the formation of a coherent bond at the phase boundary. The samples are fabricated by pressing under pressure up to 700 MPa, which reduces porosity to  $\cong 6\%$ , and sintered at  $T = 1000\text{--}1050^\circ\text{C}$ . As found out, a specific core-shell microstructure is formed in the material after sintering, where layers of TiC surround Ti grains in the composite. The thickness of the carbide layer is controlled by diffusion, and its growth at temperatures 1000 and  $1050^\circ\text{C}$  (from 5–10 mm to 10–15 mm, respectively) corresponds to the mechanism of diffusion along grain boundaries. The key stage of processing is hot forging of compacts at  $T = 1100^\circ\text{C}$ . As determined, hot forging leads to significant microstructural changes: spherical TiC inclusions are deformed and elongated in the direction of metal flow that causes mechanical anisotropy of the properties. The forging affects significant deformation strengthening and the formation of cementite ( $\text{Fe}_3\text{C}$ ). The cementite is revealed by x-ray phase analysis. In the forged samples, the combined effect of these mechanisms increases their hardness and compressive strength by  $\cong 65\text{--}70\%$  (up to 630.3 MPa). The highest hardness values are of 104–109 HRB, when combining the forging and water quenching processes. As shown, the formed heterophase structure of the Fe–Ti–C system combines a coherent adhesion between the hardening phase ( $\text{Fe}_3\text{C}$ ) and the ductile steel matrix that contributes to increased wear resistance, while the hard Ti–TiC inclusions effectively localize the abrasive impact.

**Key words:** metal–ceramic materials, titanium carbide, tool composites, thermal-deformation treatment.

У роботі досліджено вплив термодформаційного оброблення на структуру та фізико-механічні властивості металокерамічного композиційного матеріалу системи Fe–Ti–C, який було синтезовано методом *in situ* з порошкової суміші складу: Fe — 86,0%, Ti — 10,0%, графіт — 4,0%. Карбід Титану (TiC) є армованою фазою, оскільки він має високу твердість (30 ГПа), високу температуру топлення ( $\cong 3100^\circ\text{C}$ ) та низьке значення кута змочування з залізом ( $\cong 20^\circ$ ), що сприяє формуванню когерентного зв'язку на межі поділу фаз. Зразки сформовано шляхом пресування під тиском до 700 МПа, що дає змогу понизити пористість до  $\cong 6\%$ . Спінання відбувалося за  $T = 1000\text{--}1050^\circ\text{C}$ . Встановлено, що після спікання в структурі матеріалу формується характерна мікроструктура типу «ядро-оболонка», де у композитній системі зерна Ti оточено шаром TiC. Товщину карбідного прошарку обмежено дифузійними процесами, а його зростання із підвищенням температури від  $1000^\circ\text{C}$  до  $1050^\circ\text{C}$  (з 5–10 мкм до 10–15 мкм) відповідає механізму об'ємної дифузії вздовж меж зерен. Ключовим етапом оброблення є гаряче кування брикетів за  $T = 1100^\circ\text{C}$ . Визначено, що гаряче кування приводить до істотних мікроструктурних змін: сферичні вклучення TiC деформуються та витягуються в напрямку течії металу, що зумовлює виникнення механічної анізотропії властивостей. Кування впливає на значне деформаційне зміцнення й утворення цементиту ( $\text{Fe}_3\text{C}$ ). Наявність фази ( $\text{Fe}_3\text{C}$ ) підтверджується рентгенофазовою аналізою. Для кованих зразків спільний ефект зазначених механізмів

забезпечує підвищення твердості та міцності на стиск на  $\cong 65\text{--}70\%$ , досягаючи 630,3 МПа. Найвищі показники твердості складають 104–109 HRB за комбінації процесу кування та гартування у воду. Показано, що сформована гетерофазна структура системи Fe–Ti–C поєднує собою когерентний зв'язок між твердою зміцненою фазою ( $\text{Fe}_3\text{C}$ ) та пластичною металеву матрицею із криці, що сприяє підвищенню зносостійкості, а тверді включення Ti–TiC ефективно локалізують абразивне навантаження.

**Ключові слова:** металокерамічні матеріали, карбід Титану, композити інструментального призначення, термодформаційне оброблення.

*(Received 11 December, 2025; in final version, 12 December, 2025)*

## 1. INTRODUCTION

The widespread use of metal-matrix composites (MMCs) for tools that operate under friction and are subject to intense wear requires constant improvement of their properties [1–3]. Composite materials (CMs) are classified based on the morphological and structural parameters of their reinforcing components, which have different configurational features [4–6]. The CM group includes cermets or MMCs, in which the ceramic phase is a reinforcing component, and the metal phase (or alloy) is a matrix. The matrix material is aluminium, magnesium, iron, steel, or copper [7–10]. In the CMs, the metal matrix is a phase that provides ductility and strength. Therefore, the use of ceramic reinforcing components contributes to higher hardness and wear resistance of the material [11–13].

Titanium carbide (TiC) is a promising reinforcing component in a metal matrix, as it has beneficial physical and mechanical properties, including high melting point ( $\cong 3100^\circ\text{C}$ ), controlled thermal conductivity, low density ( $\cong 4.0\text{ g/cm}^3$ ), and high hardness ( $\cong 30\text{ GPa}$ ) [14]. These properties are promising for modifying the mechanical parameters of the metal matrix. The formation of target properties in the metal matrix composites (MMCs) is crucial for tool applications [15–18]. The low contact angle ( $\cong 20^\circ$ ) between titanium carbide (TiC) and iron promotes the formation of a high-quality metallic bond at the phase boundary between the ceramic-metal layer and the matrix [19]. Due to this, TiC is widely used as a reinforcing component in the production of composites for tooling and tribology applications. The possibility of local reinforcement with fine TiC particles by synthesizing them in situ and then providing their homogeneous distribution in a cast iron matrix was shown in [17]. A mixture of titanium and graphite powders was used to synthesize the reinforcing component; the molar ratio of Ti and C components was 1:1 (50 at.% Ti and 50 at.% C). The addition of the TiC ceramic phase led to an increase in CM hardness of more than

300% relative to the pure matrix alloy. In Refs. [20–23], the general properties of CMs reinforced with TiC particles and the optimization of their formation were discussed.

The use of in situ synthesis for producing CMs provides the possibility of forming gradient microstructures and core–shell structures with high hardness.

The aim of the work was to determine the effect of thermal deformation treatment and the mechanism of synthesis of the Fe–Ti–C materials for tooling on their mechanical properties and structure.

## 2. EXPERIMENTAL TECHNIQUES

According to the literature, the amount of graphite during the compaction of iron-based powder materials (PM) determined the composition of the mixture (wt.%): Fe—86.0%, Ti—10.0%, and graphite—4.0%.

Samples of 8.0 g were compacted in a cylindrical mold with a diameter of 10.0 mm. The compaction was carried out in a hydraulic press at variable pressures ranging from 200 to 700 MPa (Fig. 1).

In order to compact the samples, single- and two-stage pressing were performed [24]. With an increase in pressure from 200 to 700 MPa, the porosity of the samples decreased from 26 to 7%, respectively. Additional pressing at a pressure of 700 MPa reduced porosity to  $\cong 6\%$ , which indicated high mixture compaction. This effect is explained by

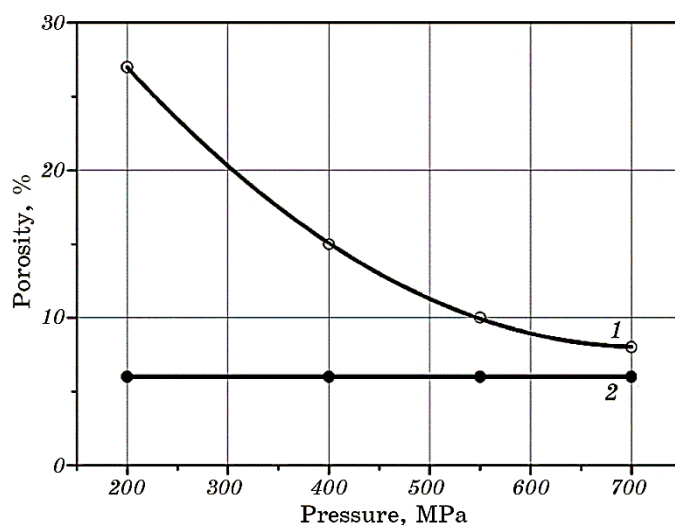


**Fig. 1.** Dependence of porosity of Fe–Ti–C-based compacts on pressure: 1—after pressing, 2—after pressing and post-pressing at 700 MPa.

the high graphite content, which reduced interparticle friction.

Sintering was carried out in a non-hermetic container at 1000–1050°C for 1 hour. After sintering, the porosity increased by 2–3%. This effect is associated with the features of titanium carbide (TiC) formation during in situ solid-phase synthesis.

In order to prevent oxidation, the thermal deformation treatment was carried out by hot forging the compacts at 1100°C with holding them in a charcoal bed for 15–20 minutes [25]. Charcoal is most often used as a solid carburizer in the cementation of steel products [26]. In this case, charcoal performs a dual function: protection against oxidation, and carbon saturation of compacts. An important feature of Fe–Ti–C system forging is the exothermic nature of the reaction of titanium carbide formation. During the synthesis, a significant amount of heat is released, which allows the sample to be kept at a high temperature for a longer time that facilitates the deformation during forging.

### 3. DISCUSSION

The CM material comprised of a steel matrix with uniformly distributed titanium carbide (TiC) inclusions. During solidification, titanium carbide formed, so the in situ synthesis occurred under stable conditions (Fig. 2).

Under particular conditions of solidification, a specific microstructure forms in the Fe (86%)–Ti (10%)–C (4%) alloy. It corresponds to the core–shell model, where each titanium grain is surrounded by a layer of titanium carbide (TiC). The formation of this microstructure is typical for materials synthesized by the reaction. This process is not equilibrium from a thermodynamic viewpoint, as it depends on two key

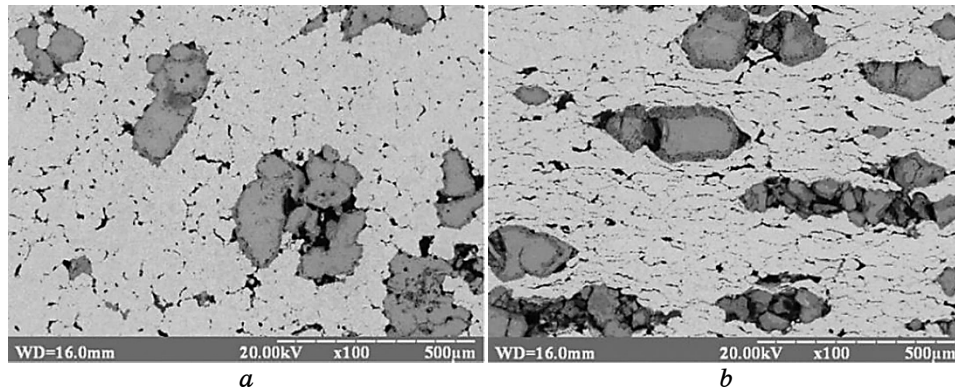


**Fig. 2.** Microstructure of Fe (86%)–Ti (10%)–C (4%) alloy after: sintering at 1050°C (*a*), sintering and hot forging at 1100°C (*b*).

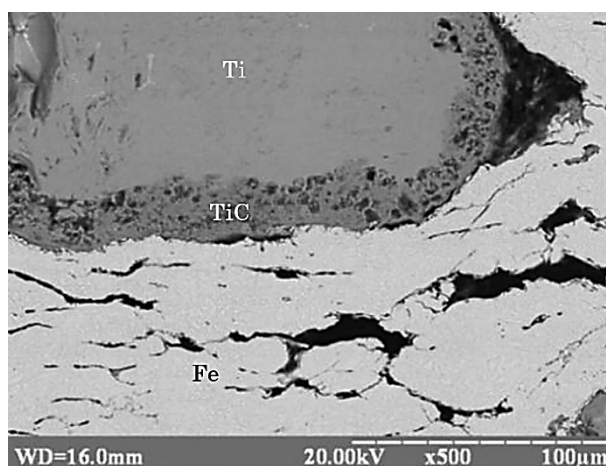


Fig. 3. Microstructure and local x-ray spectral analysis of forged sample.

TABLE 1. Results of local x-ray spectral analysis.

Spectrum	Ti, %	Fe, %
1	99.66	0.34
2	99.11	0.89
3	0.26	99.74

factors: annealing temperature and time.

The thickness of the TiC coating is determined by the diffusion along the grain boundaries. Over time, carbon atoms slowly permeate through the formed layer of titanium carbide to the titanium grains. This slows down further growth of the TiC shell, being a key factor that determines the final microstructure (Fig. 3, Table 1).

With increasing temperature, the thickness of the titanium carbide (TiC) layer forming a shell around titanium grains increased from 5–10 to 10–15  $\mu\text{m}$ . This corresponded to the features of volumetric diffusion, which intensifies at higher temperatures.

The thickness of the TiC carbide layer significantly increased after hot forging at 1100°C (up to 25–30  $\mu\text{m}$ , Fig. 4, *c*). The abovementioned data show that the temperature of forging allows effective control of both the diffusion rate and the completeness of the titanium carbide formation, which is critical for optimizing the properties of the material.

The heterophase structure of the material, formed by the developed technology, allowed for the effective distribution of mechanical loads. The main part of the impact and abrasive load was localized in the hard Ti–TiC inclusions, which ensured high wear resistance. At the same

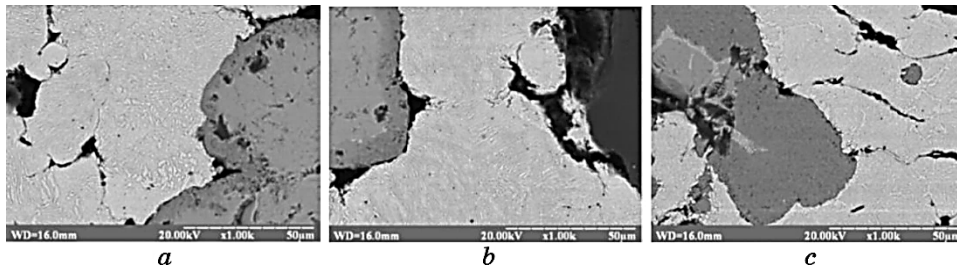


**Fig. 4.** Microstructure of Fe (86%)–Ti (10%)–C (4%) alloy after: sintering at 1000°C (*a*), sintering at 1050°C (*b*), sintering and hot forging at 1100°C (*c*).

**TABLE 2.** Hardness after loose sintering and hot forging.

No.	Treatment	Hardness, <i>HRB</i>
1	Sintered at $T = 1000^{\circ}\text{C}$	60–61
2	Sintered at $T = 1050^{\circ}\text{C}$	63–65
3	Sintered at $T = 1050^{\circ}\text{C}$ and forged at $T = 1100^{\circ}\text{C}$	85–87
4	Sintered at $T = 1050^{\circ}\text{C}$ and forged at $T = 1100^{\circ}\text{C}$ , then water quenched	104–109

time, the ductile steel matrix was an effective damper, absorbing and dissipating mechanical stresses caused by friction.

The investigation of the physical and mechanical properties of the CMs showed that the hardness of the samples largely depended on thermal and mechanical treatment (Table 2). After loose sintering, the material had a hardness of 60–65 *HRB*. The hardness increased to 80–87 *HRB* after free hot forging, which emphasizes the effectiveness of plastic deformation. The hardness reached maximum values after water quenching (104–109 *HRB*), which demonstrated the key role of the combination of mechanical and thermal treatment in optimizing the physical and mechanical properties of the CM.

After free forging, the samples had significantly higher strength and a sufficient ductility (Fig. 5, Table 3).

The forged samples had higher hardness due to the formation of cementite ( $\text{Fe}_3\text{C}$ ), caused by the diffusion of carbon from charcoal used as a filling. This was confirmed by x-ray phase analysis (see Fig. 6).

The significant increase (by 65–70%) in the strength of forged samples was caused by strain hardening, that led to a considerable increase in the microstresses, which correlated with the known values of physical and mechanical properties. Analysis of microstresses (Table 4) in individual phases of the material showed that they are compressive. After forging, the values of these compressive stresses increased by

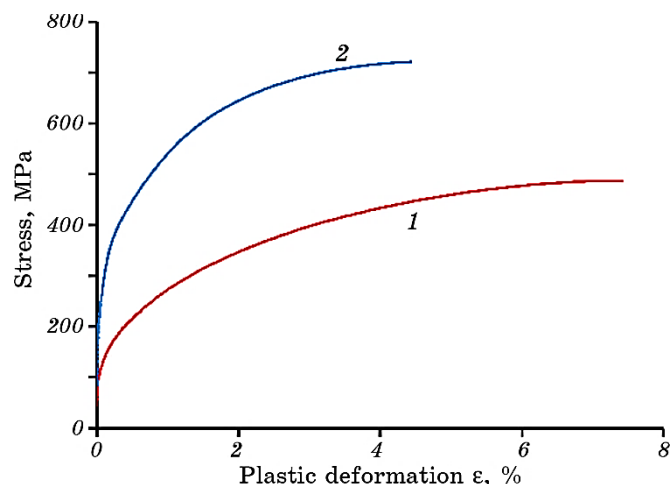


**Fig. 5.** Stress–strain curves of pressureless sintered and hot-forged samples of Fe (86%)–Ti (10%)–C (4%) alloy: 1—sintered, 2—sintered and forged.

**TABLE 3.** Mechanical properties of different samples of Fe–Ti–C system.

Treatment	No.	YS, MPa	UTS, MPa	$\epsilon$ , %
Sintering	1	179.0	467.3	0.07
Sintering and forging	2	364.2	720.8	0.05

several orders of magnitude compared to as-sintered state. The significant increase in microstresses is a result of the complex physical and mechanical action of deformation that occurred during free forging.

#### 4. CONCLUSIONS

The effect of thermal deformation treatment of the Fe (86%)–Ti (10%)–C (4%) composite system, which was produced by in situ reaction at 1100°C, led to a significant increase in the mechanical properties of the material after hot forging: hardness—104–109 *HRB*, compressive strength—720.8 MPa, and longitudinal relative deformation—0.05.

As shown, iron-based CM reinforced with TiC inclusions had a core-shell structure and a gradient microstructure of the matrix. The precipitation of TiC in the TiC–Fe ceramic layer is controlled by carbon diffusion with further formation of cementite. The high volume fraction of TiC carbide inclusions increased the wear resistance of the composite material, while the gradient structure of the TiC–Fe layer of the

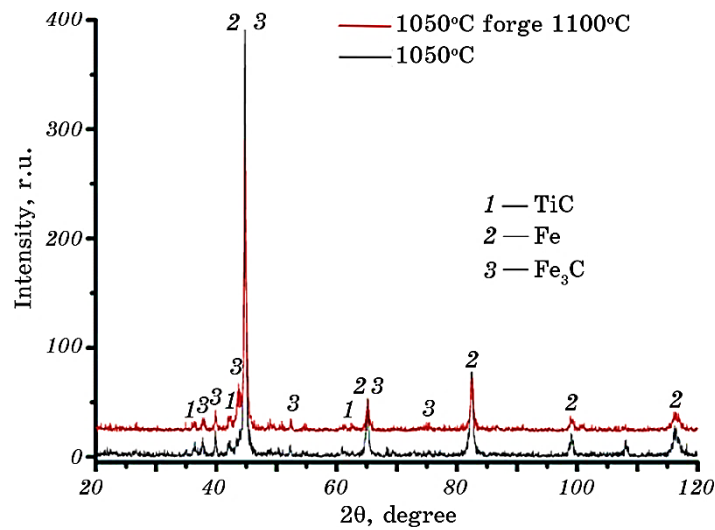


Fig. 6. X-ray phase analysis of Fe (86%)–Ti (10%)–C (4%) alloy after loose sintering and hot forging: 1—TiC, 2—Fe, 3—Fe<sub>3</sub>C.

TABLE 4. Phase composition and residual stresses in phases.

Treatment	Phase, %			Crystalline size, Å			Residual stress in phase, MPa		
	Fe	TiC	Fe <sub>3</sub> C	Fe	TiC	Fe <sub>3</sub> C	Fe	TiC	Fe <sub>3</sub> C
Sintering at 1050°C	8.2	12.82	—	261	293	—	-196 ± 645	-164 ± 671	—
Sintering at 1050°C and forging at 1100°C	88	8.9	2.7	226	153	118	-1262 ± 496	-690 ± 228	817 ± 328

cermet improved the ductility of the interface.

The feasibility of using the thermal deformation technique for manufacturing Fe–Ti–C carbide steel and the relevance of using the obtained results for producing metal–ceramic materials for tooling and tribotechnical applications are shown.

#### AUTHORS' CONTRIBUTIONS

A. V. Minitzkiy, Ye. S. Shaposhnikova, Ye. G. Byba and N. V. Minitzka provided experiment on thermal-deformation treatment, A. V. Minit-

skyi and M. Yu. Barabash contributed to the statement of the problem and the way to solve it, discussed the results and helped in preparing and approving the final manuscript. A. V. Minitzkyi, O. V. Kozlenko, V. L. Syrovatka, Ye. G. Byba, N. V. Minitzka and D. S. Leonov took part in one-sided isostatic pressing and testing of mechanical properties, contributed to the statement of the problem and discussion of the results. A. V. Minitzkyi and M. Yu. Barabash contributed to the statement of the problem and discussion of the results, took part in the formulation of problems and ways to solve it, A. V. Minitzkyi and M. Yu. Barabash analysis of x-ray phase analysis. D. S. Leonov and N. V. Minitzka participated in the task and designed it according to the requirements of article publication. All authors read and approved the final manuscript.

## REFERENCES

1. B. P. Aramide, A. P. I. Popoola, E. R. Sadiku, F. O. Aramide, T. Jamiru, and S. L. Pityana, *Wear-Resistant Metals and Composites. Handbook of Nanomaterials and Nanocomposites for Energy and Environmental Applications* (Springer: 2020), p. 1.
2. A. L. Crăciun, C. Pinca-Bretotean, C. Birtok-Băneasă, and A. Josan, *IOP Conf. Series: Mater. Sci. Eng.*, **200**: 012009 (2017).
3. L. J. Huang, L. Geng, and H.-X. Peng, *Progress Mater. Sci.*, **71**: 93 (2015).
4. F. Bouville, E. Maire, S. Meille, B. Van de Moortèle, A. J. Stevenson, and S. Deville, *Nat. Mater.*, **13**, Iss. 5: 508 (2014).
5. X. Deng, B. R. Patterson, K. K. Chawla, M. C. Koopman, Z. Fang, G. Lockwood, and A. Griffio, *Int. J. Refractory Metals Hard Mater.*, **19**, Iss. 4: 547 (2015).
6. H. X. Peng, Z. Fan, and J. R. G. Evans, *J. Microsc.*, **201**, Iss. 2: 333 (2001).
7. U. Pandey, R. Purohit, P. Agarwal, and S. K. Singh, *Mater. Today: Proc.*, **5**, Iss. 2, Part 1: 4106 (2018).
8. C. L. Wu, S. Zhang, C. H. Zhang, J. B. Zhang, and Y. Liu, *Mater. Letters*, **217**: 304 (2018).
9. F. Ma, J. Zhou, P. Liu, W. Li, X. Liu, D. Pan, W. Lu, D. Zhang, L. Wu, and X. Wei, *Mater. Characterization*, **127**: 27 (2017).
10. X. Xu, W. Li, Y. Wang, G. Dong, S. Jing, Q. Wang, Y. Feng, X. Fan, and H. Ding, *Results in Physics*, **9**: 486 (2018).
11. S. J. Algodí, J. W. Murray, P. D. Brown, and A. T. Clare, *Wear*, **402–403**: 109 (2018).
12. M. Penchal Reddy, M. A. Himyan, F. Ubaid, R. A. Shakoor, M. Vyasraj, P. Gururaj, M. Yusuf, A. M. A. Mohamed, and M. Gupta, *Ceramics Int.*, **44**, Iss. 8: 9247 (2018).
13. J. Lee, D. Lee, M. H. Song, W. Rhee, H. J. Ryu, and S. H. Hong, *J. Mater. Sci. Technol.*, **34**, Iss. 8: 1397 (2017).
14. X. Guo, M. Ma, Sh. Zhang, and Z. Wei, *J. Mater. Research Technol.*, **34**: Iss. 1–2: 761 (2025).
15. X. Cai, Y. Xu, L. Zhong, N. Zhao, and Y. Yan, *Vacuum*, **119**: 239 (2015).

16. A. Levy, A. Miriyev, A. Elliott, S. S. Babu, and N. Frage, *Mater. Design*, **118**: 198 (2017).
17. Y. Wang, X. Zhang, F. Li, and G. Zeng, *Mater. Design*, **20**, Iss. 5: 233 (1999).
18. E. Olejnik, Ł. Szymański, T. Tokarski, and M. Tumidajewicz, *Mater. Letters*, **222**: 192 (2018).
19. Y.-Z. Xing, C.-P. Jiang, and J.-M. Hao, *Vacuum*, **95**, Iss. 9: 12 (2013).
20. Z. G. Liu, J. T. Guo, L. L. Ye, G. S. Li, and Z. Q. Hu, *Applied Phys. Letters*, **65**, Iss. 21: 2666 (1994).
21. L. Zhong, Y. Xu, M. Hojamberdiev, J. Wang, and J. Wang, *Mater. Design*, **32**, Iss. 7: 3790 (2011).
22. Z. Zhao, P. Hui, T. Wang, X. Wang, Y. Xu, L. Zhong, and M. Zhao, *J. Alloys Compd.*, **745**: 637 (2018).
23. L. Zhong, X. Zhang, S. Chen, Y. Xu, H. Wu, and J. Wang, *Int. J. Refractory Metals Hard Mater.*, **57**: 42 (2016).
24. A. V. Minitzky and P. I. Loboda, *Powder Metallurgy and Metal Ceramics*, **56**, Nos. 7–8: 424 (2017).
25. A. V. Minitzky, P. I. Loboda, Ya. I. Yevych, and I. M. Zakiev, *Powder Metallurgy and Metal Ceramics*, **59**, Nos. 5–6: 290 (2020).
26. S. Supriyono and M. Mesin, *Majalah Teknik Mesin.*, **19**, No. 1: 38 (2018).